Published in final edited form as:
Biochem Biophys Res Commun. 2010 October 1; 400(4): 606–612. doi:10.1016/j.bbrc.2010.08.111.

Transforming acidic coiled-coil protein-3 (Tacc3) acts as a negative regulator of Notch signaling through binding to CDC10 / Ankyrin repeats

Sharon Bargo[*], **Ahmed Raafat**[*], **David McCurdy**, **Idean Amirjazil**, **Youmin Shu**, **June Traicoff**, **Joshua Plant**, **Barbara K. Vonderhaar**, and **Robert Callahan**[**]
Mammary Biology and Tumorigenesis Laboratory, National Cancer Institute, Bethesda, MD 20892.

Abstract

We have identified the transforming acidic coiled-coil protein-3 (Tacc3) as a binding partner for Notch4/Int3 and were able to show that it binds to the intracellular domain (ICD) of all members of the Notch receptor family. Members of the Tacc family reside at the centrosomes and associates with microtubules. Recent studies suggest that Tacc3 also contributes to the regulation of gene transcription. Tacc3 specifically interacts with the Notch4/Int3 CDC10/Ankyrin repeats and to a lesser extent, with residues C-terminal to these repeats in the ICD. Dual label immunofluorescence of mouse mammary tissue shows Tacc3 co-localizes with the Notch3 ICD. Co-immunoprecipitation of endogenous Notch and Tacc3 proteins from NIH 3T3 cell extracts, lung and mammary gland confirms that these two proteins interact under physiological conditions. In addition, knock down of Tacc3 in NIH 3T3 cells leads to the up-regulation of Hey2, a target gene for Notch signaling. The affinity of Tacc3 binding to Notch4/Int3 ICD is similar to that between Rbpj and Notch4/Int3 ICD. Notch4/Int3 ICD-Tacc3 interaction results in the inhibition of transcription from a Hes1-Luciferase reporter vector in COS-1 cells. The inhibition was reversed in these cells by increasing the levels of Rbpj. Taken together, these results suggest that Tacc3 is a negative regulator of the Notch signaling pathway.

Keywords

Taac3; Notch; CDC-10/Ankyrin repeats; protein-protein interaction; yeast two-hybrid

Introduction

The Notch4 gene was identified as a target for insertional mutagenesis by mouse mammary tumor virus (MMTV) (1,2). Integration of MMTV into Notch4 activates the expression of the portion of the gene encoding the intracellular domain (ICD) which has been designated Int3 (1,2). The ICD of Notch family members is comprised of three functionally defined regions (3): the RAM23 region located adjacent to the transmembrane domain and binds the

[*]Corresponding author, Robert Callahan, Ph.D., Mammary Biology and Tumorigenesis Laboratory, National Cancer Institute, National Institutes of Health, 37 Convent Drive, Bldg. 37, Rm. 1118, tel (301) 496-9871, fax (301) 402-0711, rc54d@nih.gov.
[*]Contributed equally

transcription repressor Rbpj (Suppressor of Hairless, Su(H)), CDC10/Ankyrin repeats, and the PEST region. The Notch family of transmembrane receptors mediates cell fate decisions throughout development (4). The Notch proteins are normally activated after interaction of the extracellular domain with one of multiple ligands and through proteolytic cleavage that results in translocation of the ICD to the nucleus where it binds to the transcription repressor Rbpj. This interaction leads to the displacement of a complex of co-repressors, and the activation of transcription of target genes. Thus MMTV integration into Notch4 represents a gain of function mutation in which the gene product, Int3, corresponds to the activated form of Notch4. In the nucleus, Int3 mediates transcription of genes associated with blocking mammary gland development and mammary tumorigenesis (4). In other studies, Int3 has been shown to mediate branching morphogenesis in mammary epithelial cells (5,6) as well as mediating vascular patterning (7,8) and inhibiting angiogenesis (9). Other studies (4) imply that there are components of Notch signaling that are independent of the Notch/ Rbpj interaction. To define potential downstream components of the Notch4/Int3 signaling pathway, we performed a yeast two-hybrid system screen (10) to identify proteins that directly interact with Int3. In this analysis we have identified the gene encoding the transforming acidic coiled-coil protein 3 (designated Tacc3) (11) as a novel binding partner for Int3 that acts as a negative regulator of Notch signaling.

Materials and Methods

Yeast Two-Hybrid and Mammalian Expression Vectors

Polymerase chain reaction (PCR) generated fragments of Notch−1, −2, −3, and −4 (Figure 1A) and RBP-J were cloned into pAS2.1 or pGAD424 (ClonTech Laboratories; Palo Alto, CA). Tacc3 DNA was PCR amplified from full-length cDNA (Invitrogen), three fragments of Tacc3 (Figure 1B) were cloned into the prey vector (pGAD424) to determine the minimal region required for binding to Notch4/Int3 1.2 protein in the yeast two-hybrid system. Cloning of each of these fragments is described in details in (Suppl. 1)

Yeast two-hybrid screen

A bait vector (pAS2.1) containing Notch4/Int3 1.2 (N4-1.2) cDNA (Figure 1A) was first confirmed to lack the ability to autoactivate histidine expression. This vector was then co-transformed with the Matchmaker mouse kidney cDNA library constructed in the prey vector (pGAD424) into *S. cerevisiae* strain Y190, (Clontech; Palo Alto, CA). Nucleotide sequence of two positive colonies showed that one encoded a portion of the Notch2 ICD (spans bases 5398-6477, (GenBank accession number D32210), and the other was Tacc3.

A Quantitative β-Galactosidase Assay

Interactions between the bait and prey vectors was measured using a β-galactosidase (β-gal) assay. Liquid synthetic dropout (SD) medium lacking leucine and tryptophan (LT) was inoculated with mated yeast colonies from SD-LT plates and incubated overnight. An equal cell number was pelleted and resuspended in 0.5ml Z buffer (Clontech Laboratories, Inc.). After freeze/thawing, 0.1ml of *o*-nitrophenyl β-D-galactopyranoside (4 mg/ml in H_2O) was added, the mixture was incubated at 30°C until yellow color appeared and the reaction was stopped. Cell debris was removed by centrifugation and the OD420 was recorded. β-gal activities are expressed as Miller units: 100X OD420/(T X V OD600), where T=time of incubation in minutes and V=volume of cell suspension. Assays were performed in triplicate.

Quantitative RT-PCR Analysis

Total RNA was prepared from a pool of mammary tissue from three FVB/N mice using TRIzol (Invitrogen). Total RNA was subjected to RT-PCR amplification using TaqMan One-Step RT-

PCR Master Mix reagents (Applied Biosystems, Foster City, CA). Tacc3, Hey2 and glyceraldehyde-3- phosphate dehydrogenase (*Gapdh*) probes were obtained from Applied Biosystems. Reactions were run in four to six replicates in an MX3000 multiplex quantitative PCR system (Stratagene). The relative abundance of mammary gland Tacc3 RNA was calculated as the ratio normalized to *Gapdh* RNA expression in mammary tissue.

Immunofluorescence

Frozen tissue sections of mammary gland were blocked with 1% PBS-BSA before primary antibody treatment. Anti-Tacc3 (Santa Cruz sc-5887) diluted 100X and anti Notch3 (Santa Cruz, Biotechnology; Santa Cruz, CA) antibody diluted 100X in the blocking buffer were used. Appropriate fluorescein-conjugated secondary antibody was used according to the manufacturer's recommendations. Cells immunocytochemistry on cells was performed as previously described (12).

RT-PCR Analysis

RNA extracts were prepared from COS-1 and NIH3T3 cells, using TRIzol (Invitrogen). Nucleotide sequence of Tacc3 specific synthetic oligonucleotides are as follows: 5'-AGTGAATTCATGCTTTCAGCTTCCACAAGT – 3' and 5'-AGC TGCGGCCGCTGATGGGTCTCTGAAGCTCT-3'; and for NOTCH4/Int3 as fellows: -GAGGACAACATTGGTCTTAAG and 5'- AGCGCGGTCTGGCTGATT. Superscript One-Step RT-PCR with Platinum Taq (Life Technologies) was used according to the manufacturer's protocol.

Transient Transfection and Luciferase Reporter Assay

COS-1 cells were cultured in DMEM medium containing 10% fetal bovine serum cell transfection and luciferase assay were performed as previously described (12).

Immunoprecipitation and Western Blot Analysis

Tissue lysates were mixed with Notch3 antibody (Millipore 07-188) or Tacc3 antibody (Santa Cruz Biotechnology; Santa Cruz, CA) for immunoprecipitation. The immunoprecipitates were analyzed by western blot analysis as previously described (13) using the tissue lysate and anti-Tacc-3 (Santa Cruz sc5885), anti-Notch4 (UpState, 07-189), anti Notch3 (Millipore 07-188) or anti-Rbpj (Santa Cruz, sc28713).

Statistics

All data are expressed as the mean ± SEM. The statistical significance of the difference between groups was determined using Student's *t* test or ANOVA as appropriate. $P \leq 0.05$ was chosen for significance.

Results

Int3 interacts with Tacc3 in the yeast two-hybrid system

A yeast two-hybrid "bait" vector expressing the portion of the mouse Notch4/Int3 ICD comprised of the Rbpj binding region (RAM23) and the CDC10/Ankyrin repeats, designated N4-1.2 terminates at a Pst1 site just C-terminal to the ankyrin repeats, was used to screen a "prey" mouse kidney cDNA library (Figure 1A). Approximately 2×10^7 transformants were screened and 2 clones were found to interacted with Int3. Nucleotide sequence analysis of these clones identified a portion of mouse Tacc3 (11) as a binding partner of Notch4/Int3 ICD (compare Figure 1Ba and 1Bb). The sequence of the protein encoded by the prey gene was identical to amino acid residues 91 to 552 (Figure 1Bb) of ERIC1 (erythropoietininduced cDNA1)/Tacc3 (14) and Tacc3a from mouse testis and ovarian cDNA libraries (14).

To further define the minimal region of Int3 required for binding Tacc3, several deletion variants of the Int3 (Figure 1A) were subcloned into "bait" vectors. Interaction between these bait proteins and Tacc3 was measured by β-galactosidase activity. The CDC10/Ankyrin region of the Notch ICD was primarily responsible for interacting with the Tacc3 protein encoded by "prey" vector (Figure 1C) since the Int3 deletion proteins lacking the CDC10/Ankyrin repeats, i.e. the RAM23 (N4-0.3) or PEST (N4-1.1) showed weak or no interaction, respectively with Tacc3. We have compared Tacc3 binding to Int3 with Rbpj, a protein known to bind to the Notch ICD (3). As shown in Figure 1C, Rbpj binds to the product of the DNA fragment encoding the RAM23 region of Int3 (N4- 0.3) and binding is enhanced when the CDC10/ Ankyrin region (N4-1.2) is also present. In addition, Tacc3 interacts with the RAM23-CDC10/ Ankyrin repeat regions (N-0.9) of Notch-2, and Notch-3 (Figure 1A). In this assay the Notch-1 ICD is self-activating (15). As negative controls, Tacc3 showed no interaction with the unrelated proteins Int6 (16), p53 (16), TAX1 (17), TAT1 or TAT2 (18) (Figure 1C). To further define the region of Tacc3 which binds to the Notch4/Int3 CDC10/Ankyrin repeats, vectors expressing Tacc3 deletions (Figure 1Bc) were tested for their interaction with Int3-1.2 in the yeast two-hybrid system. None of the proteins expressed by these deletion constructs interacted with Int3-1.2 (data not shown).

The expression and co-localization of Tacc and Notch3 in the mammary gland

In the adult mouse, expression of the 2.4 Kb Tacc3 mRNA species was highest in the testis, spleen and lung (data not shown and 7,19). In the mouse mammary gland, expression levels for *Tacc* mRNA varied dramatically with the developmental stage and *Tacc* gene (Figure 2A). Levels of *Tacc1* and *Tacc2* mRNA were highest throughout mammary development. However, unlike *Tacc2, Tacc1* expression decreased markedly during lactation. The highest levels of *Tacc1 and Tacc2* mRNA were detected in the involuted and lactating mice mammary glands respectively. Interestingly, steady state levels of Tacc3 mRNA are highest in the mammary glands of 5 wk old nulliparous and pregnant females when the gland is in an active growth phase and low in lactating and early involuted mammary glands (Figure 2A).

Tacc3 binds to the ICD of each member of the Notch receptor family (Figure 1C). To demonstrate that Tacc3 co-localizes *in vivo* with a member of the Notch receptor family we have used double-labeled immunohistochemical analysis of Tacc3 and Notch3 in mammary gland tissue of 5 wk old nulliparous, 5 day pregnant and 7 day involuted mice. Tacc3 and Notch3 showed nuclear localization in the 7 day involuted mammary gland (Suppl. Fig 1A). However, Notch3 and Tacc3 showed cytoplasmic staining in 5 wk nulliparous and 5-day pregnant (data not shown) mammary glands. Scince all cells were positive for Tacc3 in the tested mammary developmental stages, it was possible that the Tacc3 expression per cell was different. To address this question, Tacc3 immunofluorescein intensity was quantified. This analysis showed significant differences in Tacc3 cellular content in the 5 wk nulliparous and 5 day pregnant mammary gland versus the 7 day involuted mammary gland (Suppl. Fig 1B). To further substantiate the Notch3- Tacc3 interaction in normal tissue, mammary and lung tissue were collected from 10- week old FVB mice. Tissue lysates were subjected to immunoprecipitation with Tacc3 or Notch3 antibodies. Western blot of the immunoprecipitates were probed with anti-Tacc3 or anti-Notch3 antibodies. Immunostaining analysis revealed a predominant interaction between Tacc3 and Notch4 (Figure 2B). For a control, a lung lysate was loaded in the polyacrylamide gel

In vivo physical interaction between Tacc3 and Notch4/Int3

To demonstrate that in culture under physiological conditions Tacc3 physically interacts with the ICD of a member of the Notch receptor family we screened several cell lines. Tacc3 and Notch4 mRNA and protein could be detected in NIH3T3 cells but not in COS-1 cells (Suppl.

Fig 2A). In addition, Tacc3 was co-immunoprecipitated with Notch4/Int3 confirming the interaction of these proteins (Suppl. Fig 2B).

We have further characterized this interaction by comparing the relative binding efficiency of Tacc3 to Int3 with that of a known Notch ICD binding partner, Rbpj. The Tacc3 and Rbpj proteins are similar in size 637 and 500 amino acids, respectively. Protein extracts were prepared from COS-1 cells that were co-transfected transiently with fixed concentrations of the Int3 expression vector and with increasing levels of the Tacc3 expression vector. Densitometric analysis (Figure 3Ae) of western blots of the whole cell lysate confirmed the fixed levels of Int3 (Figure 3Aa) and the increasing levels of Tacc3 (Figure 3Ab). Whole cell lysates were immunoprecipitated with the Int3 polyclonal rabbit antibody and western blot analysis was performed on the immunoprecipitate using a polyclonal antibody against mouse Tacc3 (Figure 3Ac). As the concentration of Tacc3 vector was increased the level of Tacc3-Int3 binding increased (Figure 3A, compare panels b and c and their respective densitometric histograms). We analyzed under similar conditions, Rbpj binding to Int3 in COS-1 cells. As in the previous experiment COS-1 cells were co-transfected transiently with a fixed concentration of the Int3 expression vector (Figure 3B) and increasing levels of the Rbpj expression vector (Figure 3Bb). Western blot analysis of the anti-Int3 immunoprecipitate for Rbpj indicated that increasing levels of Rbpj expression vector are associated with increased levels of Rbpj binding to Int3 (Figure 3B, compare panel b and c and their respective densitometry histograms, Panel e). This suggests that the binding of Tacc3 and Rbpj to Int3 is stoichiometrically similar (compare Figure 3a and 3b panel c).

Induction and regulation of Notch4/Int3 signaling in NIH3T3 cells by Tacc3

To investigate the effect of Tacc3 and Notch interaction on Notch signaling, NIH3T3 cells were transfected with increasing levels of Tacc3 -siRNA (3, 6, and 12 μg, respectively). Quantitative RT-PCR analysis of Tacc3 expression showed a decrease in the Tacc3 expression as the Tacc3-siRNA increased. At 12 μg of Tacc3-siRNA there was a 85% decrease in Tacc3 mRNA (Suppl. Fig 3). Interestingly, Hey2 expression increased in the same cells as the Tacc3 expression decreased in a dose-dependent manner. At 12μg of Tacc3-siRNA, Hey2 mRNA expression increased 4 fold (Suppl. Fig 3). This is consistant with Tacc3 being an inhibitor of Rbpj dependent signaling. To support this hypothesis we next determined whether the Tacc3/Int3 interaction affected Int3/Rbpj signaling. This was examined in COS-1 cells transfected with Hes1-Luc reporter construct. Co-transfection of a constant concentration of the Int3 expression vector with increasing levels of the Tacc3 expression vector led to a dose-dependent down-regulation of Int3/Rbpj transcription activity from the HES1 promoter (Figure 4A). Fifty percent inhibition was achieved with 0.05 μg of the Tacc3 expression vector. In this assay it is possible that Tacc3 was competing with the binding of endogenous Rbpj (from COS-1 cells) to Int3 leading to an inhibition of Notch signaling. To test this hypothesis, we co-transfected a constant level of Int3 (0.3μg) and Tacc3 (0.1μg) expression vectors with increasing concentrations of the Rbpj expression vector. As the level of the Rbpj vector increased, Notch signaling was restored (Figure 4B). These results are consistent with a strong correlation between the ability of Tacc3 to bind Notch-ICD and its ability to down-regulate the activity of the Notch transcriptional complex.

Discussion

We have identified Tacc3 as a binding partner of Notch4/Int3. The minimal binding region (91-552 amino acid residues) for Tacc3 spans the seven acidic repeat sequences and the first coil of the coiled-coil (Tacc conserved region) region. In addition, we were able to show that, at least in the context of the yeast two-hybrid system, Tacc3 also binds to the other members of the Notch receptor family and that binding is localized to the RAM23-CDC10/Ankyrin

repeats of the ICD. Tacc proteins are ubiquitously expressed in mouse tissue. We show that the steady state levels of Tacc3 mRNA increases in the mammary gland as the ductal epithelium fills the nulliparous fat pad and then increases again during pregnancy as the density of alveolar/lobular structures expands in the gland and is subsequently down-regulated during lactation and early involution. At the onset of pregnancy, a dramatic increase in proliferation and differentiation of the mammary epithelium occurs. It is possible that the high levels of Tacc3 in the pregnant mouse mammary gland bind to Notch-ICD preventing it from binding to Rbpj. This results in the release of Notch induced inhibition of differentiation and mammary alveolar structures are formed. After parturition and with the establishment of lactation, the mammary epithelium becomes differentiated and proliferation ceases. Tacc3 expression is up-regulated during the early stages of differentiation and is down regulated in terminally differentiated cells. Involution in the mouse mammary gland is characterized by a massive loss of secretory epithelial cells resulting from programmed cell death. Tacc3 expression is at its lowest level in the involuting mammary gland. Tacc3 deficiency is associated with a high rate of apoptosis (20).

Although Tacc3 does not appear to have a nuclear localization signal sequence, PSORT II analysis predicts that there is a 76.7% probability that Tacc3 is a nuclear protein and in fact it has been found in the nucleus of interphase cells in several human and mouse tissues (19). Dual immunofluorescence of tissue sections from the mammary gland at day7 of involution, showed cells in which Tacc3 and Notch3 co-localized either to the nucleus or to the cytoplasm. The subcellular location of Tacc3 may therefore be dependent on the cell type, stage of the cell cycle, and the nature of other proteins with which it can interact. Evidence that Tacc3 and Notch3 physically interact under physiological conditions is provided by immunoprecipitation/immuno-blotting experiments with NIH3T3, mammary gland and lung protein extracts. We have used Notch3 in the immuno-precipitation experiments since Notch3 levels in the mouse mammary gland are the highest among the Notch receptors (our unpublished observation). Also, our data shows that Tacc3 interacts with all of the Notch receptors. We have also demonstrated that the affinity of Tacc3 for Notch4/Int3 is similar to the affinity of the known binding partner Rbpj for Notch4/Int3. Taken together, these data are consistent with the conclusion that Tacc3 is a binding partner of the Notch ICD.

Tacc3 has previously been identified using the yeast two-hybrid system as a binding partner to the signal transducer and activator of transcription 5 (STAT5) (20), the aryl hydrocarbon nuclear receptor translocator (ARNT) (21), and Friend of GATA-1 (FOG-1) suggesting that Tacc3 has several biological functions in the cell in addition to those involved with mitosis. In the case of ARNT and FOG-1, Tacc3 inhibits their activity by sequestering them in the cytoplasm. In this regard Tacc3 has been shown to have an essential role during development. Tacc3 is required for hematopoeitic stem cell function and genetically interfaces with p53-regulated apoptosis (20). A knock out of Tacc3 results in embryonic lethality in mice (20). In other studies Tacc3 has been shown to be associated with osteoblast differentiation (22) and is induced by erythropoietin in erythroid precursor cells (23).

Several transcription activators have been shown to interact with the histone acetyltransferases (HAT) such as the coactivator p300/CBP (24) and PCAF (25). Interestingly, mNotch1 ICD has been shown to bind to the GCN5 and PCAF HATs (26). Further, these authors showed that Notch/HAT interaction augments Notch/ Rbpj signaling and that the binding region for HAT corresponds to the CDC10/Ankyrin repeats and the transactivation (TAD) domain. Recent studies have demonstrated that human Tacc3 also binds to the hGCN5L2 and PCAF HATs (27,28). In the present study we have shown that Tacc3 inhibits, in a dose dependent manner, Int3/ Rbpj transcription of the Hes1 reporter gene. This inhibition could be relieved with increasing levels of Rbpj. These results suggest a model in which Tacc3 acts as an inhibitor of Notch signaling by displacing HAT and/or Rbpj from Int3.

Supplementary Material

Refer to Web version on PubMed Central for supplementary material.

Acknowledgments

We are indebted to K.T. Jeang (NIAID, NIH) for the TAX1, TAT1, and TAT2 expression vectors, and Dr. Ryoichiro Kageyama (Kyoto University) for the Hes-1 luciferase vector. This research was supported by the Intramural Research Program of the NIH, National Cancer Institute, Center for Cancer Research.

References

1. Gallahan D, Callahan R. The mouse mammary tumor associated gene INT3 is a unique member of the NOTCH gene family (NOTCH4). Oncogene 1997;14:1883–1890. [PubMed: 9150355]
2. Robbins J, Blondel BJ, Gallahan D, et al. Mouse mammary tumor gene int-3: a member of the notch gene family transforms mammary epithelial cells. J Virol 1992;66:2594–2599. [PubMed: 1312643]
3. Callahan R, Raafat A. Notch signaling in mammary gland tumorigenesis. J Mammary Gland Biol Neoplasia 2001;6:23–36. [PubMed: 11467450]
4. Callahan R, Egan SE. Notch signaling in mammary development and oncogenesis. J Mammary Gland Biol Neoplasia 2004;9:145–163. [PubMed: 15300010]
5. Soriano JV, Uyttendaele H, Kitajewski J, et al. Expression of an activated Notch4(int-3) oncoprotein disrupts morphogenesis and induces an invasive phenotype in mammary epithelial cells in vitro. Int J Cancer 2000;86:652–659. [PubMed: 10797286]
6. Uyttendaele H, Soriano JV, Montesano R, et al. Notch4 and Wnt-1 proteins function to regulate branching morphogenesis of mammary epithelial cells in an opposing fashion. Dev Biol 1998;196:204–217. [PubMed: 9576833]
7. Uyttendaele H, Ho J, Rossant J, Kitajewski J. Vascular patterning defects associated with expression of activated Notch4 in embryonic endothelium. Proc Natl Acad Sci U S A 2001;98:5643–5648. [PubMed: 11344305]
8. Uyttendaele H, Marazzi G, Wu G, et al. Notch4/int-3, a mammary protooncogene, is an endothelial cell-specific mammalian Notch gene. Development 1996;122:2251–2259. [PubMed: 8681805]
9. Leong KG, Hu X, Li L, Noseda M, et al. Activated Notch4 inhibits angiogenesis: role of beta 1-integrin activation. Mol Cell Biol 2002;22:2830–2841. [PubMed: 11909975]
10. Fields S, Song O. A novel genetic system to detect protein-protein interactions. Nature 1989;340:245–246. [PubMed: 2547163]
11. Still IH, Vince P, Cowell JK. The third member of the transforming acidic coiled coil-containing gene family, TACC3, maps in 4p16, close to translocation breakpoints in multiple myeloma, and is upregulated in various cancer cell lines. Genomics 1999;58:165–170. [PubMed: 10366448]
12. Raafat A, Bargo S, Anver MR, Callahan R. Mammary development and tumorigenesis in mice expressing a truncated human Notch4?Int3 intracellular domain (h-Int3). Oncogene 2004;16:9401–9407. [PubMed: 15531924]
13. Raafat A, Zoltan-Jones A, Strizzi L, Bargo S, Kimura K, Salomon D, Callahan R. Kit and PDGFR-alpha activities are necessary for Notch4/Int3-induced tumorigenesis. Oncogene 2007;26:662–672. [PubMed: 16878155]
14. Hao Z, Stoler MH, Sen B, et al. TACC3 expression and localization in the murine egg and ovary. Mol Reprod Dev 2002;63:291–299. [PubMed: 12237944]
15. Kurooka H, Kuroda K, Honjo T. Roles of the ankyrin repeats and C-terminal region of the mouse notch1 intracellular region. Nucleic Acids Res 1998;26:5448–5455. [PubMed: 9826771]
16. Merlo GR, Venesio T, Taverna D, et al. Growth suppression of normal mammary epithelial cells by wild-type p53. Oncogene 1994;9:443–453. [PubMed: 8290256]
17. Radonovich M, Jeang KT. Activation of the human T-cell leukemia virus type I long terminal repeat by 12-O-tetradecanoylphorbol-13-acetate and by tax (p40x) occurs through similar but functionally distinct target sequences. J Virol 1989;63:2987–2994. [PubMed: 2786091]

18. Trinh DP, Brown KM, Jeang KT. Epithelin/granulin growth factors: extracellular cofactors for HIV-1 and HIV-2 Tat proteins. Biochem Biophys Res Commun 1999;256:299–306. [PubMed: 10079180]

19. Aitola M, Sadek CM, Gustafsson, et al. Aint/Tacc3 is highly expressed in proliferating mouse tissues during development, spermatogenesis, and oogenesis. J Histochem Cytochem 2003;51:455–469. [PubMed: 12642624]

20. Piekorz RP, Hoffmeyer A, Duntsch CD, et al. The centrosomal protein TACC3 is essential for hematopoietic stem cell function and genetically interfaces with p53-regulated apoptosis. EMBO J 2002;21:653–664. [PubMed: 11847113]

21. Sadek CM, Jalaguier S, Feeney EP, et al. Isolation and characterization of AINT: a novel ARNT interacting protein expressed during murine embryonic development. Mech Dev 2000;97:13–26. [PubMed: 11025203]

22. Raouf A, Seth A. Discovery of osteoblast-associated genes using cDNA microarrays. Bone 2002;30:463–471. [PubMed: 11882459]

23. McKeveney PJ, Hodges VM, Mullan RN, et al.) Characterization and localization of expression of an erythropoietin-induced gene, ERIC-1/TACC3, identified in erythroid precursor cells. Br J Haematol 2001;112:1016–1024. [PubMed: 11298601]

24. Ogryzko VV, Schiltz RL, Russanova V, et al. The transcriptional coactivators p300 and CBP are histone acetyltransferases. Cell 1996;87:953–959. [PubMed: 8945521]

25. Yang XJ, Ogryzko VV, Nishikawa J, et al. A p300/CBP-associated factor that competes with the adenoviral oncoprotein E1A. Nature 1996;382:319–324. [PubMed: 8684459]

26. Kurooka H, Honjo T. Functional interaction between the mouse notch1 intracellular region and histone acetyltransferases PCAF and GCN5. J Biol Chem 2000;275:17211–17220. [PubMed: 10747963]

27. Angrisano T, Lembo F, Pero R, et al. TACC3 mediates the association of MBD2 with histone acetyltransferases and relieves transcriptional repression of methylated promoters. Nucleic Acids Res 2006;34:364–372. [PubMed: 16410616]

28. Gangisetty O, Lauffart B, Sondarva GV, et al. The transforming acidic coiled coil proteins interact with nuclear histone acetyltransferases. Oncogene 2004;23:2559–2563. [PubMed: 14767476]

29. Rogers S, Wells R, Rechsteiner M. Amino acid sequences common to rapidly degraded proteins: the PEST hypothesis. Science 1986;234:364–368. [PubMed: 2876518]

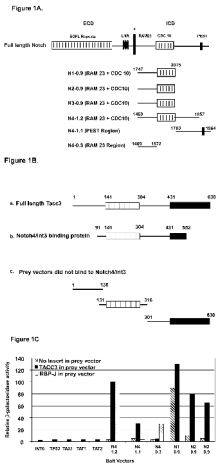

Figure 1. The interacting regions of Tacc3 and Notch/Int3 intracellular domain (ICD)

Panel A. Notch ICD deletion vectors. N1-0.9 encodes amino acid residues 1747 to 2075 of mouse Notch1 and the homologous regions of Notch2 (N2) and Notch3 (N3). Three deletion vectors of the Notch4 ICD (Int3) were constructed as described in the Materials and Methods. **Panel B**. Tacc3 deletion vectors. The numbers above the maps indicate an amino acid residue at indicated boundaries. (a) Full length Tacc3. (b) Nucleotide sequence of the gene encoding the Notch4/Int3 demonstrated that it is identical to Tacc3 gene. (c) The products of prey vectors encoding amino acid residues 1- 138, 131-316, and 301-630 did not interact with the Notch4/Int3 ICD in the yeast two-hybrid assay. **Panel C.** Characterization of the minimal regions of Notch required for intermolecular interaction with Tacc3. Tacc3 prey vector or the negative control pGAD24 vector was co-transformed by itself or with Notch bait vectors or with RBP-J expressing vector into *S. cerevisiae* strainY190. The three deletion constructs, N4-1.2, N4-1.1 and N4–0.3 were used to determine the Tacc3-binding sites within the N4/Int3 ICD. The CDC10 region of N1, N2 and N3 ICD was primarily responsible for interacting with Tacc3. The bait vectors containing Int6, TP53, TAX1, TAT1 and TAT2 represent unrelated genes that were used as negative controls.

Figure 2A

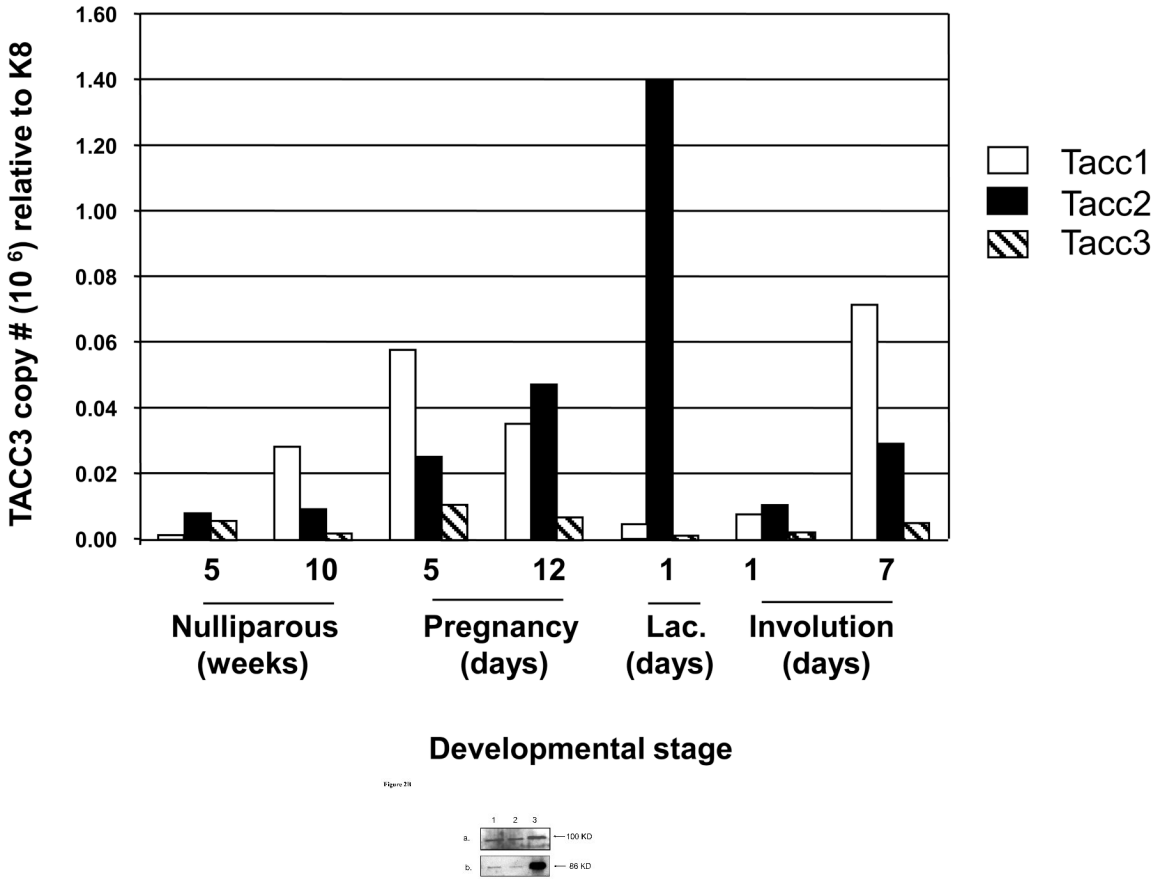

Figure 2. Tacc and Notch4/Int3 in vivo expression and co-localization

(Panel A). RT-PCR of Tacc mRNA levels in the normal mouse mammary gland. All Tacc mRNAs were expressed in the mammary gland. Tacc3 mRNA levels are the lowest in the mammary gland. Tacc1 mRNA levels peaked during early pregnancy and late involution. While, Tacc2 mRNA levels peaked in the lactating mammary gland. All reactions were performed in duplicates and repeated at least three times. The results have been normalized to the epithelial marker Kertatin 8 (K8) RNA levels. **Panel B.** *In vivo* interaction of endogenous Tacc3 with Notch3. Western blotting analysis of endogenous Notch3 and Tacc3 interaction in FVB lung (lane 1) and normal mammary gland (lane 2). Immunoprecipitation of mammary and lung protein extracts with Notch3 antibody (a) or Tacc3 antibody (b) and immunoblotting with Tacc3 antibody (a) or Notch3 antibody (b). Both Tacc3 and Notch3 were co-immunoprecipitated confirming the interaction of these proteins. Lung protein extract (lane 3) was used as a control.

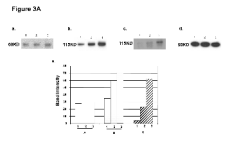

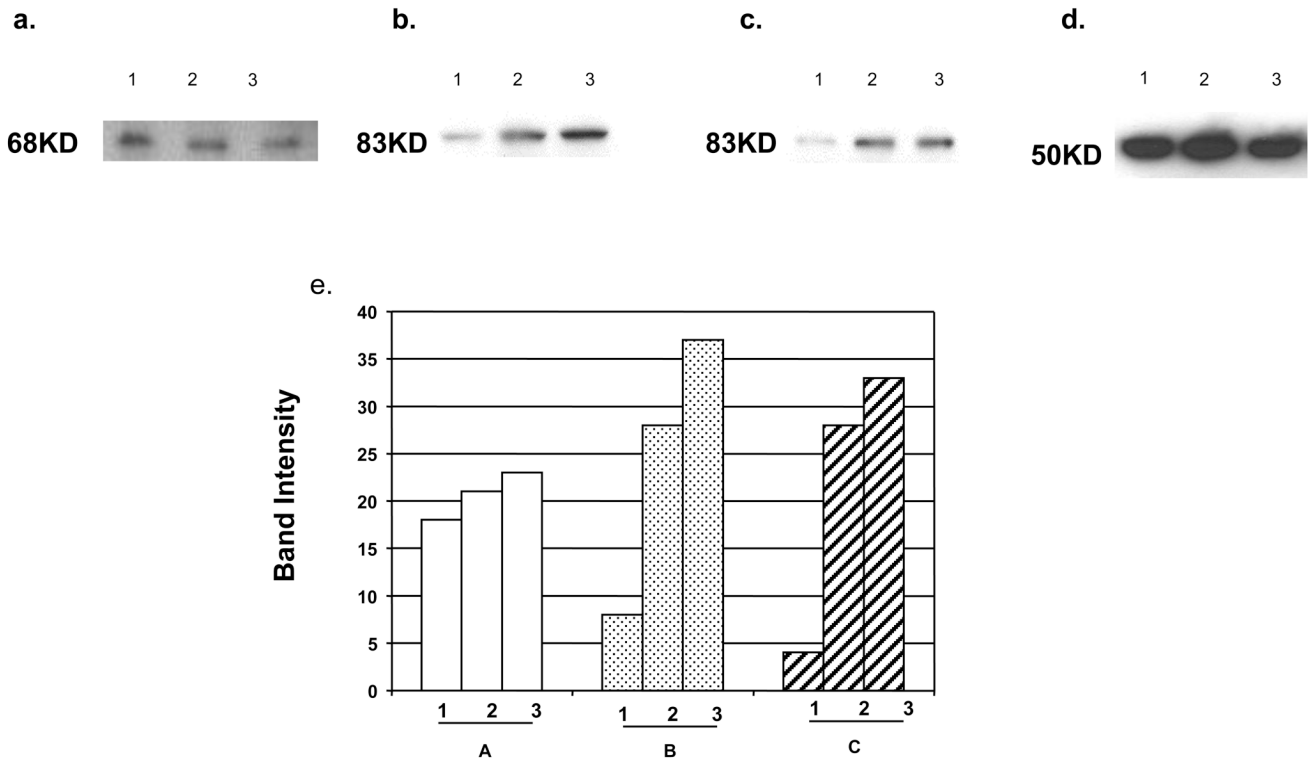

Figure 3. Interaction between Tacc3, Int3 and Rbpj in mammalian cells

Panel A. COS-1 cells were co-transfected with a fixed concentration of Int3 expression vector (0.5 μg) and increasing concentration of Tacc3 expression vector, 0.125 (lane 1), 0.25 (lane 2), 0.5 μg (lane 3). Western blot analysis of Notch4/Int3 shows constant levels of Int3 in co-transfected cells (a); and increasing levels of Tacc3 in co-transfected cells (b). Immunoprecipitates of Int3 analyzed by immunoblotting with Tacc3 antibody (c) shows an increase of Int3 binding to Tacc3 as the concentration of Tacc3 increased. Immunoblotting for α-tubulin was used as a protein loading control (d). Panel e, shows the respective measurements of band intensity in Panel a, b and c presented in arbitrary units. **Panel B.** Interaction of Rbpj with Int3 in mammalian cells. COS-1 cells were cotransfected with a fixed concentration of the Int3 vector (0.5 μg) and increasing concentration of RBP-J vector, 0.125 (lane 1), 0.25 (lane 2), 0.5 μg (lane 3). Western blot analysis of Notch4/Int3 shows constant levels of Int3 expression in co-transfected COS-1 cells (a), and increasing levels of RBP-J expression in co-transfected cells (b). Immunoprecipitates of Int3 analyzed by immunoblotting with Rbpj antibody (c), shows increasing levels of Rbpj expression vector are associated with increased levels of RBP-J binding to Int3. Immunoblotting of α-tubulin was used as a loading control for protein (d). Panel e, shows the respective measurements of band intensity in Panel A, B and C presented in arbitrary units.

Figure 4A

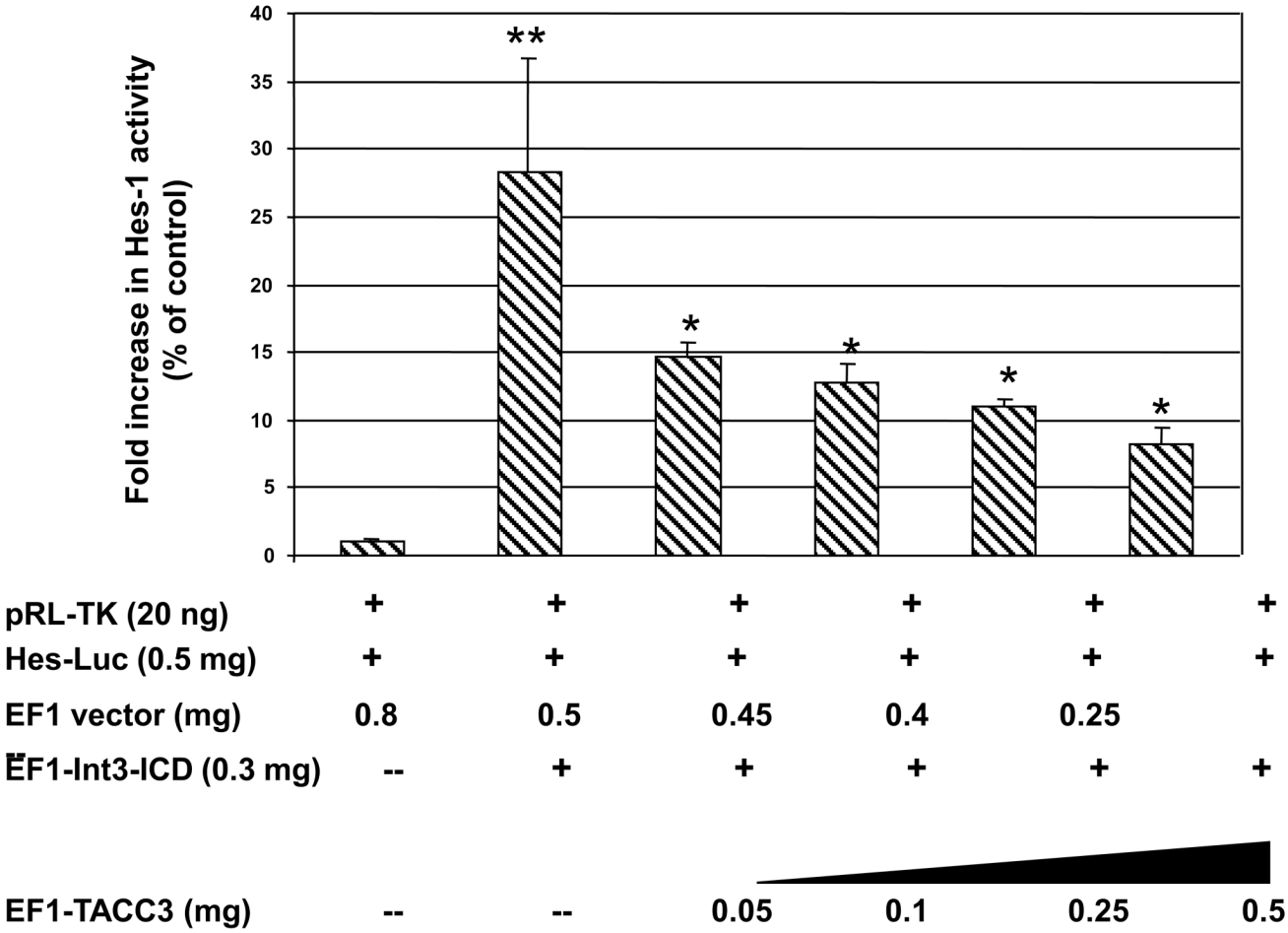

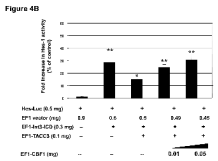

Figure 4. Regulation of Notch4/Int3 signaling by Tacc3

Panel A: COS-1 cells were transiently co-transfected with a fixed concentration of expression vectors encoding Notch/Int3 (0.3 μg) and luciferase reporter construct under the control of the Hes-1 promoter (0.5 μg) in the presence or absence of increasing concentrations of Tacc-3 expression vector (0, 0.05, 0.1, 0.25 or 0.5 μg). Data show a dose-dependent down regulation of Notch4/Int3 activation of the Hes-1 promoter as Tacc3 concentration increases. **Panel B**. COS-1 cells were transiently co-transfected with a fixed concentration of expression vectors encoding Notch4/Int3 (0.3 μg), luciferase reporter construct under the control of the Hes-1 promoter (0.5 μg), and Tacc3 (0.1 μg) in the presence or absence of increasing levels of RBP-j expression vector (0, 0.01, or 0.05 μg). Tacc3 inhibition of Int3 activity is suppressed by

increasing RBPj levels. Each bar represents the mean ± SEM of a minimum of a duplicate of three independent experiments for each experimental group. $^{**}P \leq 0.05$ compared to all treatments and $^{*}P \leq 0.05$, compared to Hes-Luc.